

Chapter 2

Fundamental Properties of Phononic Crystal

Yan Pennec and Bahram Djafari-Rouhani

2.1 Introduction to the Concept of Phononic Crystals and Their Band Structures

The control and manipulation of acoustic/elastic waves is a fundamental problem with many potential applications, especially in the field of information and communication technologies. For instance, confinement, guiding, and filtering phenomena at the scale of the wavelength are useful for signal processing, advanced nanoscale sensors, and acousto-optic on-chip devices; acoustic metamaterials, working in particular in the sub-wavelength regime can be used for efficient and broadband sound isolation as well as for imaging and super-resolution.

Phononic crystals, which are artificial materials constituted by a periodic repetition of inclusions in a matrix, are proposed to achieve these objectives via the possibility of engineering their band structures. The elastic properties, shape, and arrangement of the scatterers modify strongly the propagation of the acoustic/elastic waves in the structure. The phononic band structure and dispersion curves can then be tailored with appropriate choices of materials, crystal lattices, and topology of inclusions.

Similarly to any periodic structure, the propagation of acoustic waves in a phononic crystal is governed by the Bloch [1] or Floquet theorem from which one can derive the band structure in the corresponding Brillouin zone. The periodicity of the structures, that defines the Brillouin zone, may be in one (1D), two (2D), or three dimensions (3D). The propagation of acoustic waves in layered periodic materials or superlattices which are now being considered as 1D phononic crystals has been extensively studied [2] since the early paper of Rytov [3]. However, the

Y. Pennec • B. Djafari-Rouhani (✉)
Institut d'Electronique, de Microélectronique et de Nanotechnologie,
Université de Lille 1, IMEN Bat P5, Villeneuve d'Ascq 59655, France
e-mail: yan.pennec@univ-lille1.fr; bahram.djafari-rouhani@univ-lille1.fr

concept of phononic crystal was introduced only two decades ago in relation with 2D [4–6] and 3D [7] periodic media, especially to seek for the possibility of the so-called absolute band gaps [8–10]. Indeed, the dispersion curves exhibit band gaps in which the propagation of waves is prohibited. Such gaps may occur for particular directions of the wave vector, but they can also span the whole 2D or 3D Brillouin zone where the propagation of elastic waves becomes forbidden for any polarization and any incident angle. Then, the structure behaves like a perfect mirror for any incidence angle, thus prohibiting the transmission of sound waves.

The concept of phononic crystal followed by a few years the analogous concept of photonic crystals [11, 12] for the propagation of electromagnetic waves. The existence of band gaps is especially well-known in solid state physics in the field of electronic band structure of crystalline materials. In particular, the properties of semiconductors, such as electronic, conduction, and optical properties, are dominated by the band gap separating the valence and conduction bands and, moreover, these properties can be drastically modified and tailored by introducing defects into the semiconductor due to the emergence of new states inside the band gaps (the so-called localized modes associated with the defects which have a decaying wave function far from the defect position). Similarly, the introduction of defects such as waveguides and cavities in phononic or photonic crystals are at the origin of many of their potential applications for confinement, guiding, filtering, and multiplexing of acoustic waves at the level of the wavelength [10] and pave the way for the realization of advanced sensors and acousto-optic devices.

The progress in the field of phononic crystals goes in parallel with their photonic counterpart, although they involve a larger variety of materials as concerns the possibility of high contrast among the elastic properties, large acoustic absorption and the solid or fluid nature of the constituents. Since the band structure is scalable with the dimensions of the structure (as far as the linear elasticity theory applies), a great deal of works has been devoted to macroscopic structures in the range of sonic (kHz) and ultrasonic (MHz) frequencies where the proof of concepts of band gaps and manipulation of sound (such as wave guiding, confinement, sharp bending) have been established with simple demonstrators. Yet, there is a continuous interest in the engineering of band structures with new structures and materials as well as the technological fabrication of sub-micron scale structures working in the hypersonic (GHz) regime.

The general mechanism for the opening of a gap is based on the destructive interference of the scattered waves by the inclusions and therefore requires a high contrast between the elastic properties of the materials. In periodic structures, this is called the Bragg mechanism and the first band gap generally occurs at a frequency which is about a fraction of c/a , where c is a typical velocity of sound, and a the period of the structure. However, when the propagating waves in the embedding medium are strongly scattered by the internal resonances of the individual inclusions, one may obtain a so-called hybridization gap which results from the coupling between the propagating waves of the matrix and the localized mode of the scatterers [13, 14]. Such a gap is less sensitive to the periodicity and can persist even in presence of some disorder in the structure [15, 16]. For common

materials, it may happen that both types of gaps arise in the same frequency range since the internal resonances of the inclusions would be of the order of c/d where d is the typical diameter or size of the inclusion. In such cases, the combination of the two effects can widen the actual band gap. It is also worthwhile mentioning the concept of locally resonant sonic materials (LRSM) introduced by Ping Sheng et al. [17] which later developed into the field of acoustic metamaterials. In the latter work, the coating of hard inclusions by a very soft rubber produced a very low frequency resonance gap situated two orders of magnitude below the Bragg gap, thus allowing the sound isolation below kHz by a sample with a thickness of a few centimeters only.

Point or linear defects [18] such as cavities or waveguides [19] can be introduced into the phononic crystal by removing or modifying one, a few or a row of inclusions. Depending on their geometries and constitutions, such defects can give rise to new modes inside the band gap of the phononic crystal that correspond to localized or evanescent waves with a decaying displacement field far from the defect [20–22]. Therefore, they can be used for confinement and guiding [23, 24] of the acoustic waves and the coupling between a waveguide and cavities provide the possibility of filtering devices [25, 26, 10].

In this preliminary chapter, we limit ourselves to a basic presentation of the trends on the dispersion curves and band gaps in different types of phononic crystals with solid or fluid constituents. For the sake of simplicity, we consider only the case of 2D crystals constituted by a periodic array of infinitely long bars in a matrix background. Then, we review the localized modes associated with some simple defects and their applications in filtering and multiplexing phenomena. In a final section, we briefly summarize further developments in the field of phononic crystals.

2.2 Dispersion Curves and Band Gaps in 2D Phononic Crystals

2.2.1 *Origin of the Band Gaps: Bragg Gaps and Local Resonances*

An absolute phononic gap, if one exists, can be a Bragg type gap, which appears at about an angular frequency ω of the order of c/a where c is a typical velocity of sound in the structure and a the lattice parameter. The existence of absolute band gaps was predicted theoretically [4–8] prior to being demonstrated experimentally in various phononic crystals constituted of solid components [27, 28] or mixed solid/fluid components [29]. It has been shown that the existence and bandwidth of the gaps depend strongly on the nature of the constituent materials (solid or fluid), the contrast between the physical characteristics (density and elastic constants) of the inclusions and the matrix, the geometry of the array of inclusions, the inclusion shape and the filling factor.

It can be also a resonance type gap, which can appear at frequencies below the Bragg limit. In the latter case, it is possible to obtain absolute gaps at frequencies one to two orders of magnitude lower than the Bragg diffraction threshold, without increasing the size of the unit cell in the crystal. Such gaps can be realized in the so-called LRSM, whose building units exhibit localized resonant modes at specific frequencies [17, 30]. Forming a phononic crystal from such components, the resonances interact and give rise either to flat bands or to resonance gaps about the corresponding eigenfrequencies. As these localized resonances depend on the properties of the individual scatterers, their position in frequency can be tuned by properly choosing the properties (elastic or geometric) of the scatterer. These materials could found several potential applications, in particular in the field of sound isolation or in the realization of vibrationless environment for high precision mechanical systems, negative refraction or cloaking acoustic metamaterials.

2.2.2 Behavior of the Band Gaps as a Function of the Geometrical and Physical Parameters

Phononic crystals are heterogeneous elastic media composed of a periodic array of inclusions embedded in a matrix. The main characteristic of such composite media is to exhibit stop bands in their transmission spectra, in which the propagation of waves is forbidden. Three classes of phononic crystal can be defined, which differ from each other by the physical nature of the inclusions and the matrix. One can thus define solid–solid, fluid–fluid, and mixed solid–fluid composite phononic crystals. The opening of wide acoustic band gaps requires two main conditions. The first one is to have a large physical contrast, such as density and speed of sound, between the inclusion and the matrix. The second condition is to present a sufficient filling factor of the inclusion in the matrix unit cell. One can note that the forbidden band gap occurs in a frequency domain given by the ratio of an effective sound velocity in the composite material to the value of the lattice parameter of the periodic array of inclusions. In two-dimensional solid–solid phononic crystal, the modes of vibration can be decoupled between the in-plane propagation where the elastic displacement is perpendicular to the cylinders and the out-of-plane propagation where the elastic displacement is parallel to the cylinders axis. In fluid–fluid phononic crystals, only longitudinal modes are allowed. In mixed phononic crystals, complex modes of vibration can exist, ranging from longitudinal in the fluid to longitudinal and transverse in the solid part. In this section, we will give a few examples of the three classes of phononic crystals, dealing with the nature, the composition, and the geometry of the constituents. Most of the following calculations have been performed using improved methods such as plane wave expansion (PWE), finite difference time domain (FDTD), well-known in the field of photonic crystals, and finite element method (FEM).

Table 2.1 Mass density ρ and elastic constants C_{11} , C_{44} , and C_{12} of silicon and epoxy. $c_l = \sqrt{\frac{C_{11}}{\rho}}$ and $c_t = \sqrt{\frac{C_{44}}{\rho}}$ represent, respectively, the longitudinal and transverse speed of sound

Material	ρ (kg/m ³)	C_{11} ($\times 10^{11}$ dyn/cm ²)	C_{44} ($\times 10^{11}$ dyn/cm ²)	C_{12} ($\times 10^{11}$ dyn/cm ²)	c_l (m/s)	c_t (m/s)
Silicon	2,331	16.57	7.962	6.39	8,430	5,844
Epoxy	1,180	0.761	0.159	0.443	2,540	1,161

2.2.3 Solid–Solid Phononic Crystal

The elastic band structure of two-dimensional solid–solid composite materials has been investigated independently in a few works by Sigalas and Economou [4, 7, 31] and Kushwaha et al. [5, 6]. These authors demonstrate the existence of absolute phononic band gaps in the first irreducible Brillouin zone. The dependence of the band gap on the composition of the material and on the physical parameters of the constituents was investigated in [6, 8, 27]. In the following, we propose to examine in detail the elastic band structures and existence of absolute band gaps in phononic crystals made of two common materials, silicon and epoxy. Silicon is considered to be a cubic material with a crystallographic axis [001] parallel to the direction of propagation whereas epoxy is isotropic. The physical parameters of the two materials are reported in Table 2.1. These materials present a strong contrast between both their densities and elastic constants, meaning that silicon is the hard material while epoxy is the soft one. The first general requirement corresponding to the existence of absolute band gap is then respected.

The purpose of the section is to investigate three lattices of periodic structures, i.e. square, hexagonal, and honeycomb, as depicted in Fig. 2.1. The two-dimensional cross section of the three investigated arrays is represented, in which a is the lattice parameter. The corresponding Brillouin zone is also represented where (Γ, X, M) (resp. (Γ, J, X)) are the high symmetry points of the first irreducible Brillouin zone for the square (resp. hexagonal and honeycomb) array.

We first deal with hard material inclusions inside a soft matrix. Figure 2.2a shows one example of the dispersion curves for a square array of silicon cylinders in epoxy matrix, the filling factor defined by β being equal to 0.68. In the range of frequency of Fig. 2.2a, two complete band gaps are found for the in-plane and out-of-plane polarizations of the modes. The choice of the filling factor $\beta = 0.68$ produces almost the largest complete band gap.

Indeed, in Fig. 2.2b, the evolution of the band gap widths (white area) is presented as a function of the filling factor. The first complete band gap is the largest one and is open over a large range of filling factor, above 0.2. We note that the largest width of the band gap ($\frac{\Delta(fa)}{(fa)_{\max}} = 28\%$ at $\beta = 0.74$) is open for very high filling fraction which can be a limitation for technological fabrication. A second smaller band gap opens for $\beta > 0.55$. The central frequencies of both band gaps increase with increasing the filling factor.

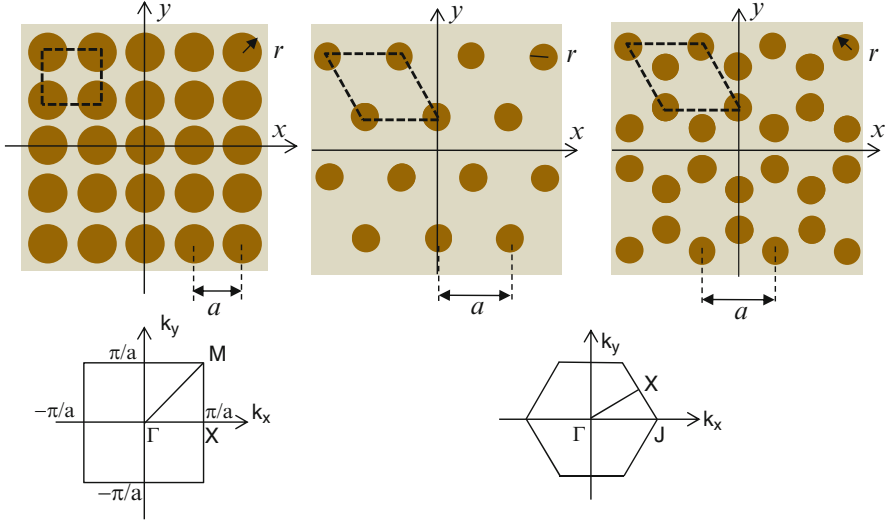


Fig. 2.1 Two-dimensional cross sections of square, hexagonal, and honeycomb lattices with the corresponding Brillouin zone. The *dashed lines* represent the elementary unit cell of lattice parameter a . r is the radius of the inclusions

In Fig. 2.2c, we present the evolution of the band gaps for the hexagonal lattice. We obtain now three band gaps where the largest opens up for a filling fraction of $\beta > 0.36$, with a maximum width ($\frac{\Delta(fa)}{(fa)_{\max}} = 37\%$) around $\beta = 0.80$.

Finally, for the honeycomb lattice, (Fig. 2.2d), a large and complete band gap opens at higher frequencies and for filling fraction in the range $0.24 < \beta < 0.44$. In this composite system, the gap width ($\frac{\Delta(fa)}{(fa)_{\max}} = 8\%$ at $\beta = 0.34$) is much lower than those obtained for the two preceding geometries. As a conclusion, for hard inclusions in a soft matrix the largest band gaps are obtained for the hexagonal and square lattices and the former allows lower filling fractions.

It is worth noticing that the band gaps are also dependent upon the shape of the inclusions. For example, we have shown [8] that their positions and widths can be changed if the circular inclusions are replaced by squares. Moreover, by rotating the squares with respect to the axes of the photonic crystals, one can also tune the band gaps.

In the opposite situation of soft epoxy inclusions in a silicon matrix, the square and hexagonal lattices display absolute band gaps only for very high filling fraction which may be not interesting from a fabrication point of view. On the contrary, for the honeycomb lattice (Fig. 2.3), one can observe the opening of an absolute band gap as far as the filling fraction exceeds $\beta = 0.34$. Moreover, the band gap width increases strongly and reaches the larger value of $\frac{\Delta(fa)}{(fa)_{\max}} = 78\%$ at $\beta = 0.60$.

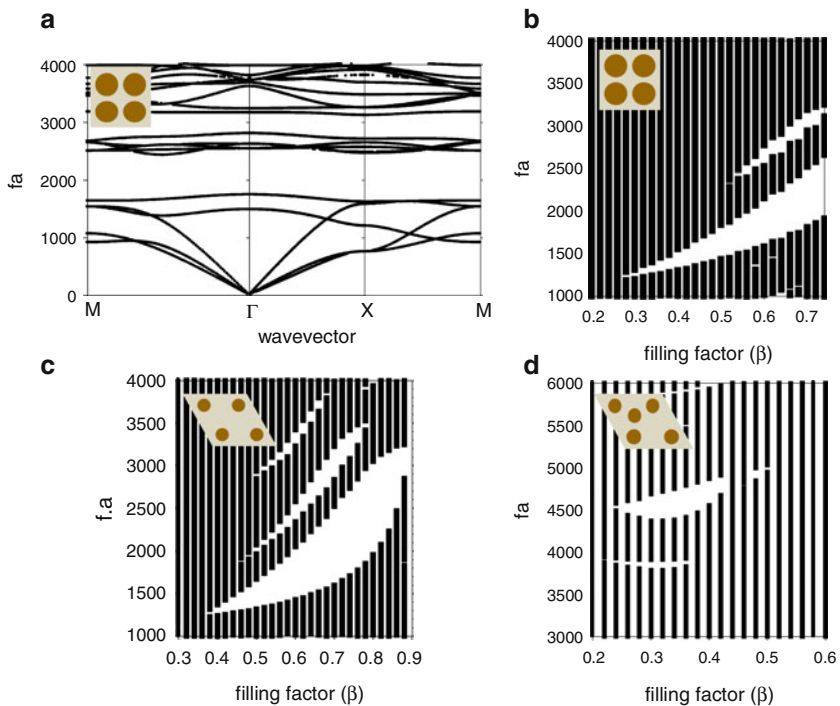


Fig. 2.2 Band gap existence in phononic crystal made of hard silicon inclusion in soft epoxy matrix. (a) Example of dispersion curve for the square array of symmetry with filling factor $\beta = 0.68$. Band gap maps for (b) square, (c) hexagonal, and (d) honeycomb arrays as a function of the filling factors

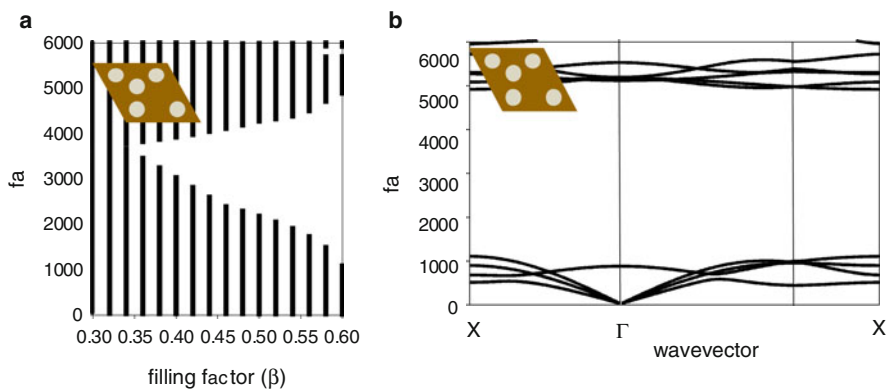


Fig. 2.3 (a) Band gap map for the honeycomb array of soft epoxy inclusions in hard silicon matrix. (b) Example of dispersion curves for the honeycomb structure with filling factor $\beta = 0.60$

Table 2.2 Mass density ρ and speed of sound of steel and water

Material	ρ (kg/m ³)	c_l (m/s)	c_t (m/s)
Steel	7,780	5,825	3,227
Water	1,000	1,490	—

2.2.4 Solid–Fluid Phononic Crystal

We now turn to solid–fluid periodic structures known as mixed phononic crystals. A large contrast in physical properties between the two materials is often satisfied particularly in the case of solid/gas combinations. The mixed systems present complex modes of vibration as the liquid allows only longitudinal modes while the solid allows both longitudinal and transverse modes. Due to this difficulty, the PWE method generally fails to predict accurately the acoustic band structures for such a mixed system. This drawback can be alleviated by imposing the condition of elastic rigidity to the solid inclusions [32, 33] which is satisfactory to describe the sound propagation in a phononic crystal made of solid inclusions in air. Nevertheless, this difficulty can be overcome by making the band structure calculations with the FDTD method [34] which allows defining the real nature of both solid and liquid [28, 35]. In the mixed systems, the fluid can be either a condensed liquid [28, 36, 37] or a gas [38–40]. We propose here to consider two different cases, i.e. when solid inclusions are inserted in a liquid matrix and the opposite situation.

We first investigate the case of a phononic crystal made of steel cylinders in a water matrix. The density and elastic constants of the two materials are given in Table 2.2. We present the calculations for the in-plane vibrations.

The left diagram of Fig. 2.4a shows the band structure along the direction ΓX of the irreducible Brillouin zone, calculated for a square array of steel cylinders of radius $r/a = 0.38$. The right part of Fig. 2.4a shows the transmission coefficient using the FDTD calculation. The incoming wave is a longitudinal pulse, uniform along the X direction and with a Gaussian profile along the Y axis. The transmitted signal is recorded as a function of time over the cross section of the waveguide, and finally Fourier transformed to obtain the transmission coefficient versus frequency. The spectrum is normalized with respect to the signal obtained without the phononic crystal sample. For the ΓX direction, the band diagram shows a large band gap from 500 m/s to almost 1,000 m/s.

We have then computed similarly the dispersion curves and transmission spectrum for hollow steel cylinder filled with water [22, 41]. The inner radius r_i/a is chosen equal to 0.22 with the same outer radius $r/a = 0.38$ as in the previous case. One can see that the insertion of the hollow tubes widens the stop band, with the upper edge of the band gap moving towards higher frequencies. But looking at the transmission spectrum, the most remarkable feature is the existence of a narrow pass band localized inside the band gap of the hollow cylindrical phononic crystal, at $fa = 780$ m/s. As the inner radius increases from 0.2 to 0.25, the frequency of the narrow pass band decreases.

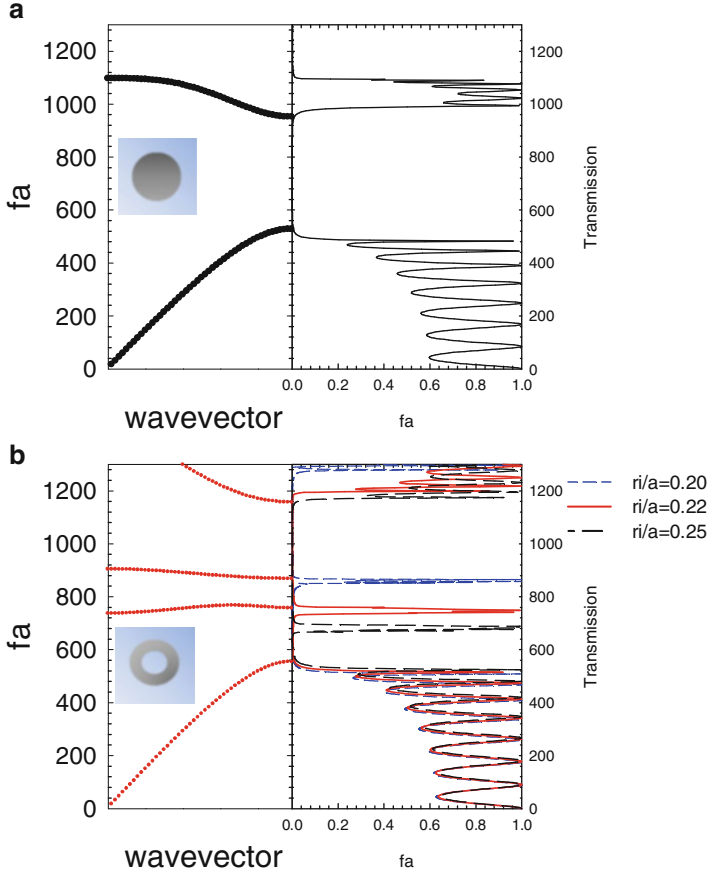
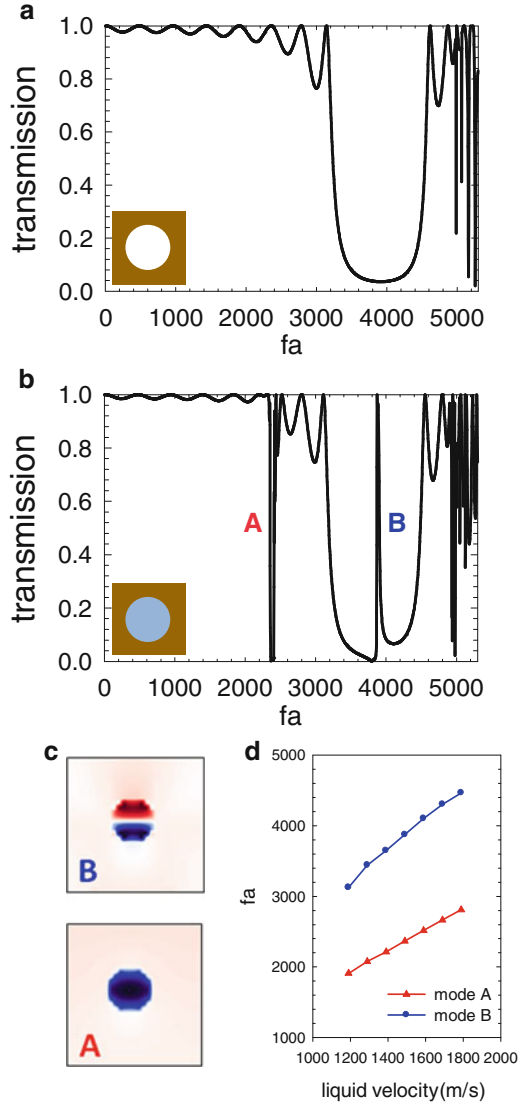


Fig. 2.4 (a) Dispersion (*left*) and transmission (*right*) curves of the phononic crystal composed of steel cylinders of radius $r/a = 0.45$ in water matrix. (b) (*Left*) Dispersion curve for hollow cylinders of inner radius $ri/a = 0.22$ and filled with water. (*Right*) Transmission curves for hollow cylinders of variable inner radius

The dispersion curves, calculated for the inner radius $r/a = 0.22$, present two flat bands inside the band gap. The lower one, at $fa = 780$ m/s, fits perfectly the narrow pass band observed in the transmission spectrum. The upper one, at 900 m/s, does not contribute to the transmission. Such a band is named a “deaf band” because it cannot be excited due to symmetry reason [42]. A detailed analysis of the eigenvectors associated with these vibration modes is reported in [43]. We have also shown that the nearly flat transmitted branch does not correspond to a mode localized in the water-filled cavities inside the hollow cylinders but to a propagative branch with very slow group velocity.

We now consider the opposite situation where the two-dimensional phononic crystal is made of water cylinders in silicon. The conclusion can be also extended to

Fig. 2.5 Transmission curve through a 2D square lattice phononic crystal made of periodic holes of radius $r/a = 0.18$ in a silicon substrate when (a) the holes are empty and (b) the holes are filled with water. (c) Map of the displacement field at the dip A and the peak B. (d) Evolution of the frequencies of the resonant modes A and B as a function of the velocity of the liquid inside the holes



the case where the cylinders are filled with a liquid polymer [44]. Figure 2.5a shows as a reference the calculation of the transmission curve when the phononic crystal is made of air holes with radius $r/a = 0.18$ inside the silicon matrix. One can see that the spectrum presents a large pass band below 3,000 m/s then a band gap between 3,000 and 4,200 m/s.

When the holes are filled with water (Fig. 2.5b), the transmission curve exhibits two new features labeled A and B, which appear as a dip in the transmitted branch and a peak in the band gap. To give a deeper insight of the two features A and B, we

calculated (Fig. 2.5c) their corresponding maps of the displacement field. The dip A and the peak B are associated with a high confinement of the field inside the water holes. Due to the large contrast between the acoustic velocities and impedances of water and silicon, these modes can be considered as cavity resonances inside the holes surrounded by an almost rigid material. Therefore, their frequencies are very close to the solution of the equation $J'_m(\omega r/c_{\text{liq}}) = 0$ where J'_m is the derivative of the Bessel function of order m , ω the frequency, r the radius of the cylinder, and c_{liq} the velocity of sound in water. In the transmission curve of Fig. 2.5b, it appears that the resonant modes of the cavity give rise, respectively, to a dip or a peak as far as their corresponding frequencies fall inside a pass band or a band gap of the phononic crystal. In Fig. 2.5d, we give the evolution of the features A and B when changing the longitudinal acoustic velocity c_{liq} of the liquid filling the holes with respect to the water. The frequencies of the resonant modes increase by increasing the sound velocity of the liquid and in both cases the relative shift in frequency ($\Delta(f)/f = 20\%$) has almost the same order of magnitude as the relative shift of the sound velocity ($\Delta c_{\text{liq}}/c_{\text{liq}} = 24\%$).

One interest of such mixed structure is to present a new way to sense the sound velocity of bio-chemical liquids [45, 46]. To make a phononic sensor, the well-defined features should display a high quality factor, be very sensitive to the acoustic velocity of the liquid, and remain relatively isolated in frequency from each other in order to allow the sensing of the probed parameter on a sufficiently broad range. Such ultra-compact structure can be shown as label-free, affinity-based acoustic nanosensor, useful for bio-sensing applications in which the amount of analyte is often limited.

2.2.5 Fluid–Fluid Phononic Crystal

In this section we assume that the materials constituting the phononic crystal are made of two different fluids. An interesting example is provided by air cylinders (in 2D) or air bubbles (in 3D) in a water matrix. Indeed, these structures display giant sonic stop bands resulting from a combination of Bragg and resonance scatterings that can be obtained whatever the symmetry of the lattice [47–49]. Figure 2.6a illustrates the transmission coefficient for a square lattice of air cylinders in water background for a filling factor $\beta = 20\%$. The lattice parameter taken equal to $a = 20$ mm in order to fall in the audible frequency range. One can see a large stop band extending from 0.5 to 20 kHz, followed by a sharp peak. Thus this system would have the property of preventing the propagation of sound in a large frequency domain, with the period of the sonic crystal being much smaller than the acoustic wavelength in air. The few peaks of transmission below 0.5 kHz come from the lowest dispersion curve. The peak A, at 20 kHz, corresponds to a mode localized inside the air cylinder (a resonance of the air cylinder), as can be seen in Fig. 2.6a. Such localization is possible due to the huge density and compressibility contrasts between air and water.

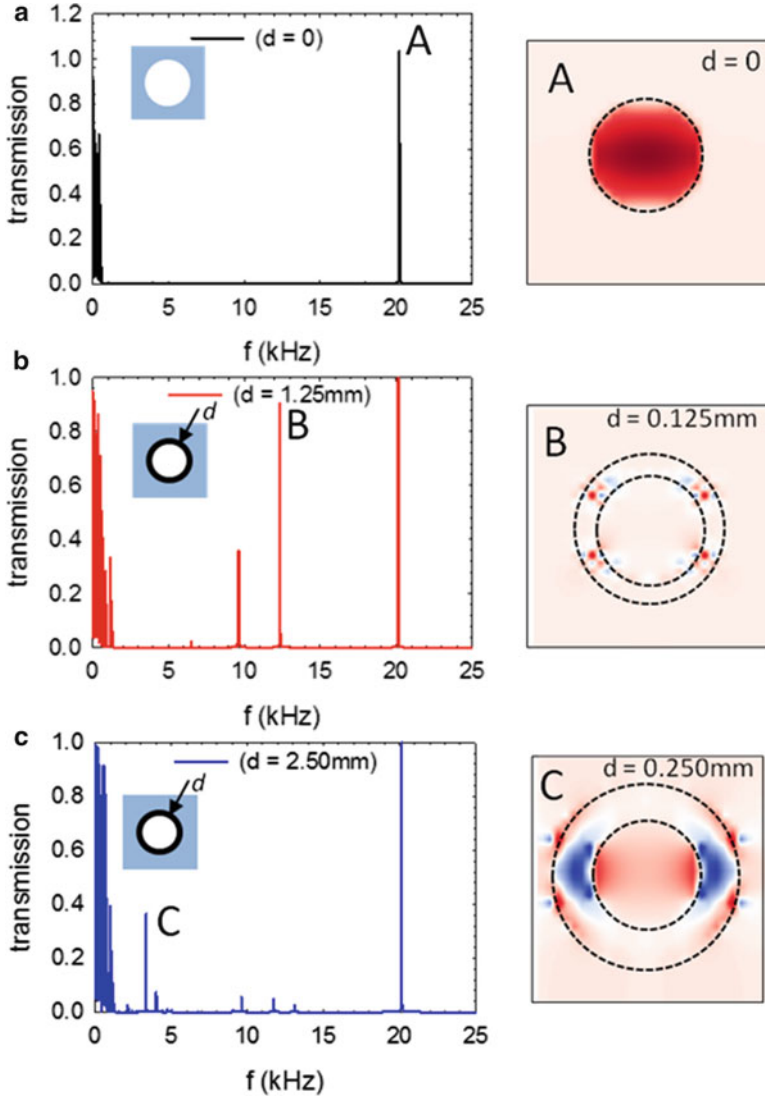


Fig. 2.6 Spectral transmission coefficient for three values of the polymer thickness: (a) $d = 0$, (b) $d = 1.25$ mm, and (c) $d = 2.50$ mm. The lattice parameter is $a = 20$ mm and the inner radius of the tube (air cylinder) is 5 mm. The maps of displacement field close to each diagram correspond to one example of the transmitted peaks

In the following, we consider the more practical system where air inside cylinders is surrounded by a thin polymer shell immersed in water. The transmission calculations are presented for different thicknesses of the polymer shell (Fig. 2.6b, c). The density and elastic constants of the two materials are reported in Table 2.3.

Table 2.3 Mass density ρ and speed of sound of air and polymer [50]

Material	ρ (kg/m ³)	c_l (m/s)	c_t (m/s)
Soft polymer	995	1,000	20
Air	1,000	340	–

In contrast to [34, 17] where the velocities of sound in the polymer were assumed very low and especially unrealistic as concerns the longitudinal velocity, here we chose realistic values of longitudinal (1,000 m/s) and low transverse (20 m/s) velocities as reported in [50]. However, the physical conclusions which are much dependent upon the transverse velocity of the polymer will remain very similar to those presented in [34].

In Fig. 2.6b (resp. c), the thickness of the polymer shell is $d = 1.25$ mm (resp. 2.50 mm), while keeping the air cylinder at $r = 5$ mm. A large and low frequency stop band is still observed but now starting at 1.2 kHz. Moreover, while the peak at 20 kHz is still present, some new ones appear in the transmission as B or C, mainly localized inside the polymer layer of the inclusion as seen in the map of the displacement fields of Fig. 2.6b, c. As a conclusion, it has been shown that hollow cylinders made of an elastically soft polymer containing air inside and arranged on a square lattice in water can still give rise to very large acoustic band gaps at low frequencies. In the opposite case of water cylinders in an air background, large band gaps can be obtained with a honeycomb lattice with a very high filling fraction (touching cylinders) [34].

2.2.6 Locally Resonant Phononic Crystal

As introduced previously, an absolute phononic gap, if one exists, can be a Bragg type gap or a resonance type gap, which can appear at frequencies well below the Bragg limit. Such structure, known as acoustic metamaterials, presents an important issue for phononic crystals related to their property of perfectly reflecting mirror for the purpose of sound isolation, negative refraction, and sub-wavelength imaging. The objective consists of finding structures that attenuate the propagation of sound over a sample whose thickness remains smaller than the wavelength in air. Most of the recent studies have been directed towards a new class of phononic crystals, the so-called locally resonant materials [17]. These structures essentially consist of a hard core, such as a metal, surrounded by a soft coating (silicone rubber) and immersed in a polymer such as epoxy. Due to the local resonances associated with the soft coating material, dips can appear in the transmission coefficient at very low frequencies situated about two orders of magnitudes below the Bragg frequency. Such behaviors have been obtained in both 3 and 2D locally resonant phononic crystals.

In this section, we present for a 2D phononic crystal, a generalization of the preceding structure to a multilayer cylindrical core constituted by two or several

coaxial shells surrounding the internal hard core [30]. The structural unit of the phononic crystal consists of an infinitely long cylinder, composed of multicoaxial shells, embedded in a water matrix. The inner (core) cylinder is made of steel. This core is coated by alternate shells constituted, respectively, by a thin layer of an elastically soft material and a thin layer of a hard material (steel). In this calculation, the soft polymer is chosen to have very small transverse velocity $c_t = 19$ m/s with a longitudinal velocity of $c_l = 55$ m/s. In the following, we fix the outer radius of the cylinder equal to 8.4 mm and the thickness of each layer in the coating equal to 1.6 mm. The filling fraction of the whole cylinder, taken to be $\beta = 55\%$, will be kept constant. Finally, the sonic crystal is constituted by five rows of elementary units arranged on a square lattice, with a lattice parameter of $a = 20$ mm, embedded in water. The whole size of the sonic crystal is therefore 10 cm.

Figure 2.7a reports the transmission through a phononic crystal made of a bi-layer inclusion constituted by a steel core coated with one polymer and one steel layer. At very low frequency, a sharp dip appears in the transmission spectrum ($f = 1.45$ kHz) for which the displacement field (Fig. 2.7b) shows an elastic field localized inside the inclusion. The displacement can be understood as a motion of the core and the outer steel layer in phase opposite each other, while the polymer acts as a spring (see the schematic representation). This behavior can be interpreted as the appearance of a dynamic negative effective mass density in the frequency range of the dip [17].

We investigate now the case of a multicoaxial cylinder containing an even number of shells, 4 and 6, and we consider that the uttermost shell in contact with water is made of steel. In this way, we obtain an alternation of hard and soft materials with a solid core. Figure 2.8a presents the low frequency transmission curves in which the number of low frequency dips evolves in relation with the number of shells. A number of 2 (resp. 3) bi-layers give rise to 2 (resp. 3) low frequency peaks.

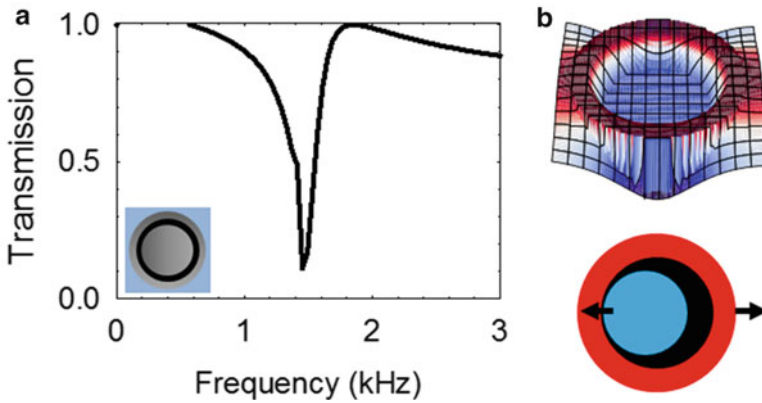


Fig. 2.7 (a) Transmission curve through a low resonant phononic crystal made of a steel core coated with a polymer and a steel layer, embedded in water. (b) Displacement field calculation at the frequency of the dip and corresponding schematic representation on the motion of the mode

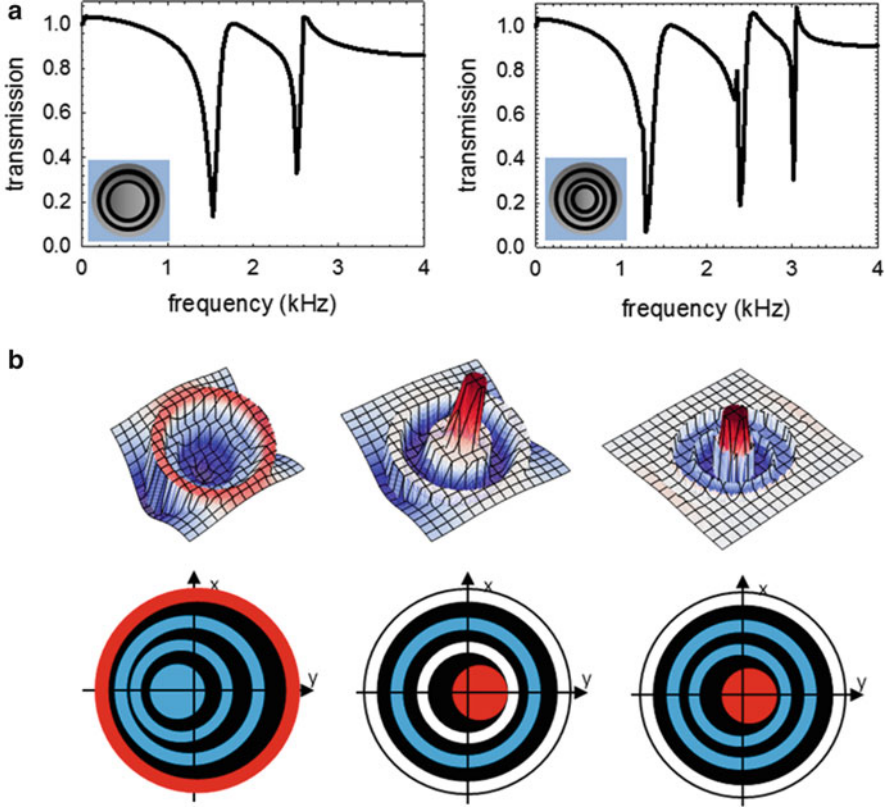


Fig. 2.8 (a) Transmission curves through a low resonant phononic crystal made of a steel core coated with 2 (*left*) and 3 (*right*) bi-layers constituted of polymer and steel, embedded in water. (b) Displacement field at the frequency of the dips for 3 bi-layers and the corresponding schematic representation of the rigid motions of the steel core and shells

Figure 2.8b gives an illustration with $N = 3$ of the displacement fields of the three resonance modes. For each frequency, we give the component of the displacement along the direction of propagation, as well as a schematic view of the vibrations. The common feature to all these three modes is the fact that the hard parts of the inclusion, namely the inner core and the three steel cylindrical shells, vibrate as rigid bodies linked together through the polymer shells that act as springs. In the lowest mode, occurring at $f = 1.61$ kHz, the inner core and the two following steel shells vibrate in phase along the propagation direction, while the outer steel shell moves with the opposite phase. The displacement fields of the second ($f = 3.0$ kHz) and third ($f = 3.77$ kHz) resonant modes correspond to other vibrational states of four rigid bodies linked together through the polymer shells. Therefore, we show the possibility of obtaining several dips in the transmission coefficient in a

given frequency range. By combining two or more phononic crystals of different parameters, we could also show that it is possible to overlap some dips and obtain a widening of the frequency gaps [30].

2.3 Localized Modes Associated with Defects

2.3.1 Guiding

The existence of band gaps in phononic crystals may be useful for the purpose of introducing functionalities such as waveguiding and filtering in integrated structures. The ability to tailor the acoustic properties of phononic crystals and more specifically of their waveguides makes them particularly suitable for a wide range of applications from transducer technology to filtering and guidance of acoustic waves. They can operate at the frequencies of telecommunications (about 1 GHz) when the lattice parameter of the phononic crystal is in the micron range. This section is dealing with some examples of the properties of linear and point defects in phononic crystals such as wave bending and splitting [24, 52] or transmission through perfect or defect-containing waveguides [19, 23, 53].

As a basic structure, we consider a mixed (solid/fluid) 2D phononic crystal composed of steel cylinders in a water matrix. The inclusions are arranged periodically on a square lattice. Throughout this section, we assume the lattice parameter $a = 3$ mm and the radius of the inclusion $r = 1.25$ mm resulting in a filling factor $\beta = 0.55$. This insures that the phononic crystal displays a large absolute band gap of Bragg type in the ultrasonic range, extending from 250 to 325 kHz. All numerical simulations are based on the finite difference time-domain (FDTD) method.

We first investigate the properties of the phononic crystal containing a simple straight waveguide obtained by removing one row of cylinders along the direction of propagation (Fig. 2.9a). We have calculated the transmission through the guide as a function of the frequency. As seen in Fig. 2.9a, the guide exhibits a full transmission band in the frequency range (270–300 kHz) that covers a large part of the phononic crystal stop band. The map of the displacement field corresponding to the frequency 290 kHz shows that the transmission can be associated with a high confinement of the field inside the waveguide.

One can also demonstrate the bending of acoustic wave constructed by removing holes over a large frequency range inside the absolute band gap of the perfect phononic crystal [24]. Figure 2.9b shows the transmission curve obtained through the bending waveguide formed by two sharp corners with 90° angle. We show that most of the linear guided modes are transmitted except a transmission dips at 275 kHz. Figure 2.9b shows a numerical illustration of the propagation of the wave at 290 kHz through the bending waveguide in which the incident wave propagates along the first straight waveguide, couples successfully with the perpendicular one, then reaches to the last horizontal one.

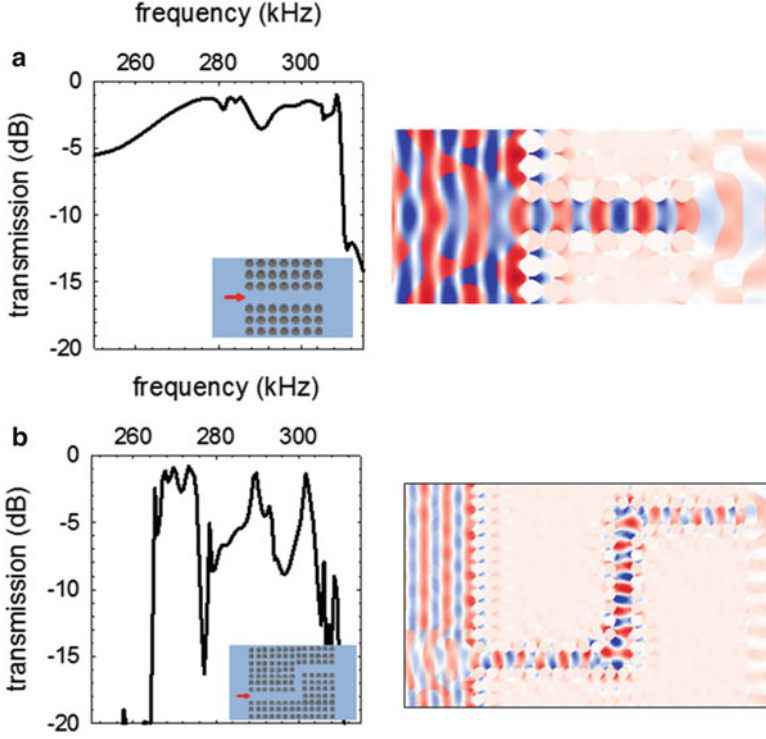


Fig. 2.9 Calculated transmission spectra in the frequency range of the band gap and displacement fields at $f = 290$ kHz through (a) a straight and (b) a bent waveguide

2.3.2 Filtering

We now turn to the behavior of the phononic crystal where a point defect is inserted inside the waveguide. A resonant cavity (or stub) of nominal length and width equal to one period is simply obtained by removing one cylindrical inclusion attached to the guide as sketched in the insert of Fig. 2.10a. As compared to Fig. 2.9a, the transmission remains almost unchanged except for one narrow dip occurring at the frequency of 290 kHz where the transmission becomes very small. It clearly appears that in the presence of a stub the transmission through the waveguide can be significantly altered due to the interference phenomena. In Fig. 2.10a we have represented the map of the displacement field at the frequency of the dip. One can see the wave entering the guide, penetrates into the stub, reflects at the end of the stub, and then returns back to the entrance of the guide while the transmission towards the end of the guide remains negligible. The eigenmodes of the cavity have been used advantageously to induce a very narrow stopping band in the pass band of the waveguide.

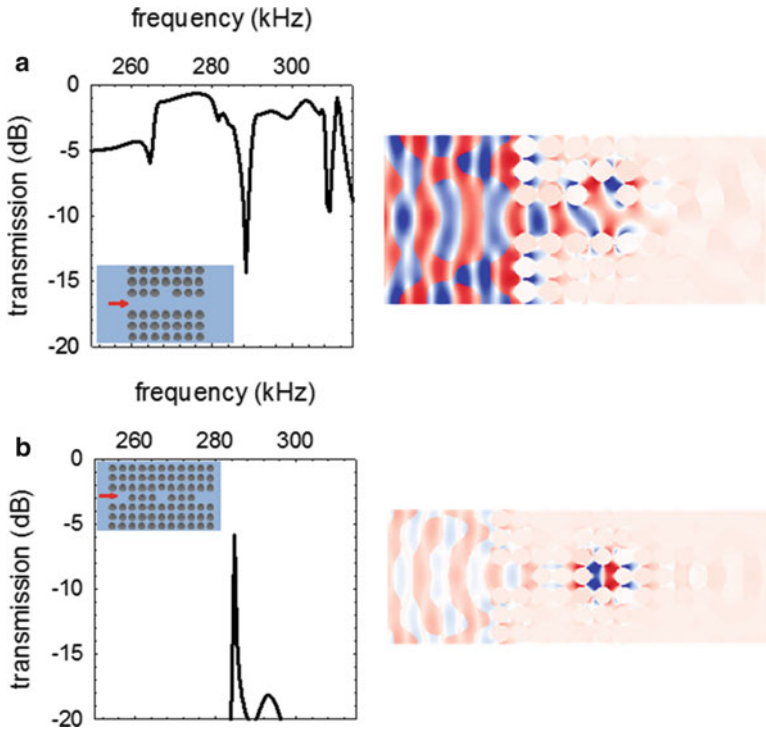


Fig. 2.10 Calculated transmission spectra in the frequency range of the band gap and displacement fields at the frequency of the dip (resp. peak) when a cavity is inserted (a) at the side of the guide or (b) inside the waveguide

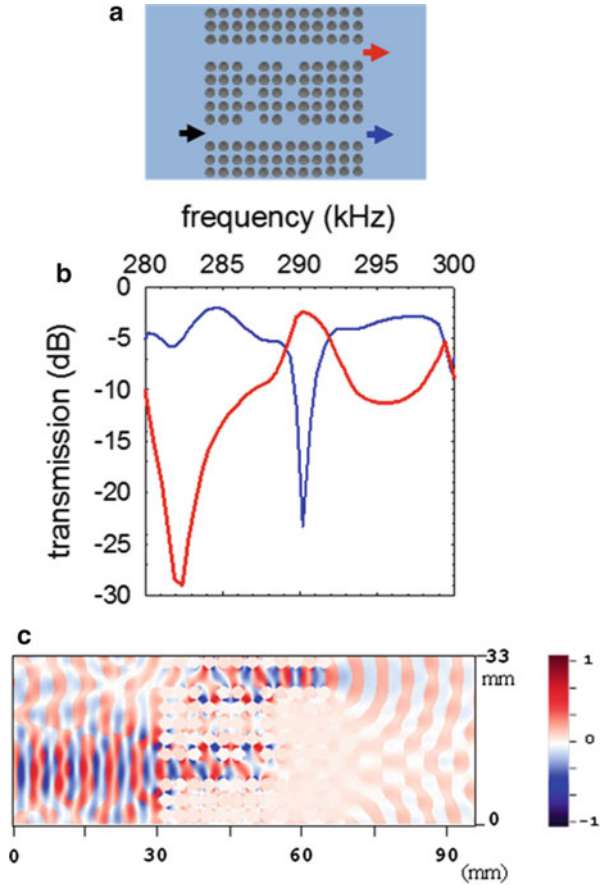
In Fig. 2.10b, we have considered the same cavity incorporated inside the waveguide. The cavity is isolated from the entrance and the exit of the waveguide by three steel cylinders. Nevertheless, the transmission spectrum exhibits a peak which occurs at the resonance frequency of the cavity. This transmission is due to a coupling between the cavity modes and the waveguide one, via tunneling effects. Indeed, a single cavity incorporated into the waveguide limits the transmission mainly to the frequencies situated in the neighborhood of the eigenfrequencies of the cavity.

So, the same cavity can have two opposite effects depending on whether it is incorporated inside or at the side of the waveguide, leading, respectively, to applications as transmitted selective or rejective filters.

2.3.3 Demultiplexing

Based on the previous results, we have studied an acoustic channel drop tunneling in a phononic crystal, i.e., the possibility of transferring one particular acoustic wavelength between two parallel waveguides coupled through an appropriate coupling element which is composed of two coupled cavities interacting with stubs located at the sides of the two parallel guides (see Fig. 2.11a) [26]. The incoming wave is a longitudinal pulse with a Gaussian profile which only covers the entrance of port 1 (black arrow), leaving port 4 essentially unaffected. The transmitted signals, displayed in Fig. 2.11b, are recorded at ports 2 (blue arrow) and 3 (red arrow). It can be observed that the direct transmission at port 2 drops almost to zero at the frequency of 290 kHz. At the same time, a significant peak of transmission occurs at port 3, with a magnitude comparable to the loss at port 2. This means that, at this frequency, the incoming signal is essentially transferred to the second wave

Fig. 2.11 (a) Schematic view of the phononic crystal with two waveguides coupled through an element constituted by two vacancies. Stubs along the guides ensure the efficiency of the coupling. The black, red, and blue arrows indicate the entrance and exit signal. (b) Calculated transmission spectra at the output ports for an input Gaussian signal coming from port 1. At the frequency of 290 kHz, the incident wave drops from the first to the second waveguide. (c) Calculated displacement field along the direction of propagation at a frequency of 290 kHz, averaged over one period of oscillation. The red color (blue) corresponds to the highest (lowest) value of the displacement field given in arbitrary units



guide towards port 3, leaving all other exits of the structure unaffected. In other words, the input signal tunneled through the coupling element and dropped inside the second wave guide.

To obtain a direct confirmation of the demultiplexing phenomenon, the FDTD computation was used to simulate a monochromatic source at the frequency of 290 kHz. The computed displacement field along the direction of propagation is displayed in Fig. 2.11c. The transfer of the input signal from port 1 to port 3 is clearly apparent together with an absence of signal at port 2.

2.3.4 Tunability

The tunability can be achieved by a modification of the geometrical parameters, the nature of the constituents [22, 41] or by an external physical stimulus applied to the phononic crystal. The purpose of the tunability is to modify some specific properties of the phononic crystal such as the band gap width or the position of singular features.

In Sect. 2.4, we have investigated the case of a two-dimensional phononic crystal that incorporates a narrow pass band inside a band gap. They are constituted of a periodic repetition of hollow cylinders filled and immersed in water. As seen in Fig. 2.4b, the position of the narrow pass band is quite sensible to the value of the inner radius, r_i of the inclusions. The modification of the frequency of the narrow pass band has been also investigated when the hollow cylinders are filled with a fluid other than water. We chose mercury because of the large contrast between its physical parameters and those of water. In Fig. 2.12a, we report the transmission coefficient through the phononic crystal with hollow cylinders with inner radius $r_i/a = 0.22$, filled with water or mercury and we clearly notice the shift of the frequency of the narrow pass band.

Figure 2.12b summarizes the values of the frequencies for a set of inner radius. One can conclude that the narrow pass band can be tuned and may offer a mean for selective transmission. The value of the frequency can be adjusted both by changing the inner radius of the cylinders or the nature of the fluid that fills them. In the latter case, the tuning of the frequency can be made either in a passive way or actively by injecting and flushing the fluids contained in the interior of the cylinders.

We can also combine tunability and guiding by design phononic crystals waveguides with narrow pass band. We will discuss the multiplexing and demultiplexing properties of Y-shaped waveguides constituted of hollow cylinders. Let us consider sketched in Fig. 2.13a. The structure is constituted by a heteroradii waveguide with alternating radii $r_i/a = 0.24$ and $r_i/a = 0.20$ then divided at its end into two branches. Each branch is constituted of hollow cylinders designed for the propagation of waves with only one frequency corresponding to one specific narrow pass band.

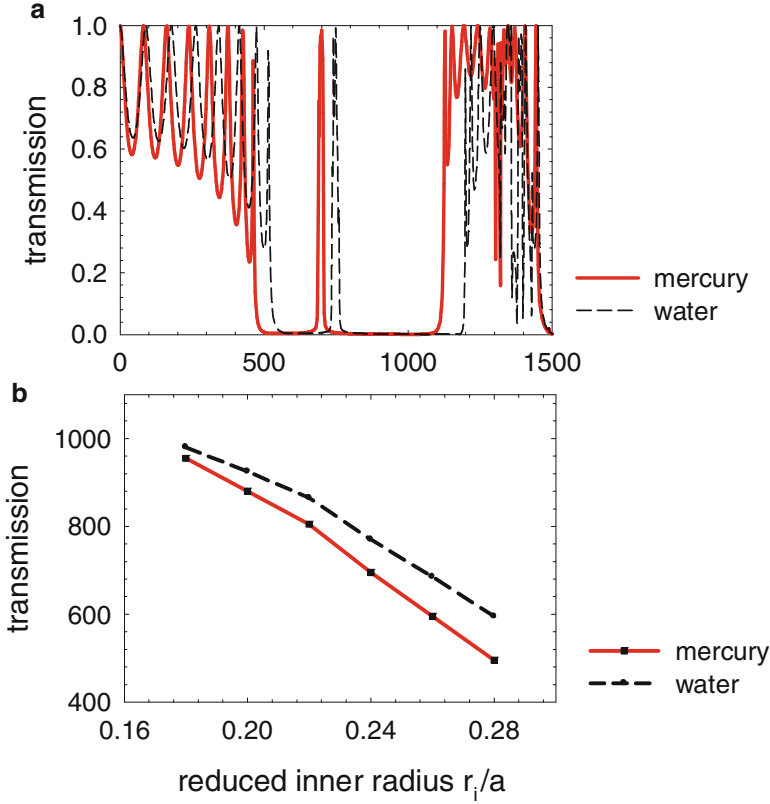
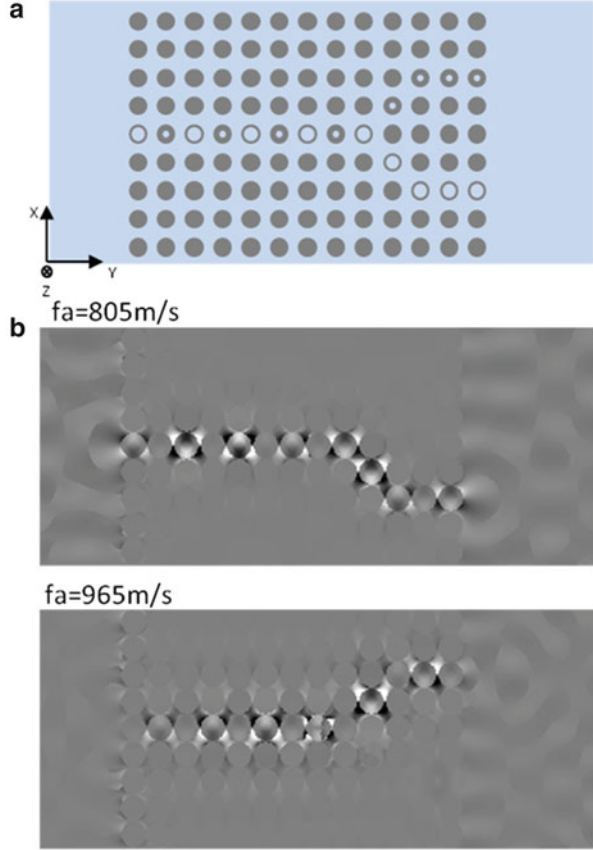


Fig. 2.12 (a) Transmission spectra calculated for a phononic crystal composed of hollow cylinders with inner radius $r_i/a = 0.22$ containing mercury (solid red line) or water (dashed black lines). (b) Values of the narrow pass band centered frequencies for phononic crystals of hollow cylinders with different inner radius containing mercury or water

We launch at the entrance of the structure a monochromatic excitation at the value of frequency of the narrow pass band corresponding to $r_i/a = 0.24$ and $r_i/a = 0.20$. One can see on the displacement field calculations of Fig. 2.13 that each frequency is guided through the heteroradii waveguide and then directed towards the branch corresponding to the respective inner radius. It means that, when an initial broad band signal is sent from the right of the system, each branch of the Y-shaped waveguide will select its own narrow pass band. These two signals are then superimposed into the heteroradii waveguide. As a result, the transmitted spectrum will contain two peaks corresponding to both narrow pass band and selectively transmitted. Finally, similar conclusions hold if the Y-shaped waveguide contains hollow cylinders of same inner radius filled with two different fluids [41].

Fig. 2.13 (a) Schematic representation of the Y-shaped waveguide. The left part of the waveguide contains two types of cylinders with inner radii $r_1/a = 0.24$ and $r_1/a = 0.20$, in alternation. Each branch of the Y contains one type of cylinder to permit the separation of the two narrow pass bands. (b) Representation of the displacement field for a Y-shaped waveguide at the two frequencies of $fa = 805$ and 965 m/s



2.4 Concluding Remarks and Further Developments in the Field of Phononic Crystals

The main object of this chapter was to present the basic results about the trends of the dispersion curves and band gaps in phononic crystals, as well as the emergence of localized modes associated with cavities and waveguides and their functionalities in acoustic devices. Another type of localized modes which will be described in detail in a next chapter concerns the surface acoustic modes when the phononic crystal is cut along a plane. Besides the surface modes of lamellar materials (or superlattices) that have been widely studied [54, 2], an early paper presented the Rayleigh waves and their folding when a superlattice is cut normal to the laminations [55]. Later, the surface modes of a 2D phononic crystal cut perpendicular to the cylinders were calculated [56, 57] and then observed experimentally a few years after [58–61]. The possibility of an absolute gap in the

band structure of surface waves was also demonstrated [62, 59]. Other works studied the surface waves of a 2D crystal cut parallel to the cylinders [63] or of a 3D crystal composed of spheres in a matrix [64].

Phononic crystals of finite thickness, such as a periodic array of holes in a plate or a periodic array of pillars on a membrane, started to be studied during the last decade. It was demonstrated that they can also exhibit absolute band gaps, thus providing the same functionalities associated with defects as in infinite phononic crystals. In the case of periodic holes in a plate [65, 66], the existence of an absolute band gap requires having a thickness of the slab about half of the period. In the case of periodic pillars on a membrane [67–70], besides the possibility of wide Bragg gaps, a low frequency gap exhibiting metamaterial type behavior can be obtained with an appropriate choice of the geometrical parameters [67, 70], in particular a small thickness of the membrane. With the advancements of nanotechnologies, there is a great deal of interest on nanophononics [71, 72], in particular phononic circuits with waveguides and cavities inside sub-micron phononic membranes working at a few GHz.

In this paper, we briefly mentioned examples of tunable phononic crystal where the band structure can be modified by changing the geometrical parameters (for instance, rotating square shape inclusions [8, 51]) or material parameters (for instance, filling hollow inclusions [41]). More generally, such modifications can be induced dynamically by the application of external stimuli, for instance an electric or magnetic field with piezoelectric or magnetoelastic materials [73–76], a stress in elastomeric structures [77], or the change of temperature [78, 79] (for example, the phase transitions of a polymer infiltrating the holes of a phononic crystal).

A new emerging topic concerns the search of dual phononic and photonic band gap materials in which the phonon–photon interaction can be drastically enhanced with the simultaneous confinement of both electromagnetic and acoustic waves [80–82]. For instance, stimulated Brillouin scattering can be expected over a short distance in a so-called phoxonic membrane while in general it happens in fibers which are several meters long. The optomechanic interaction between phonons and photons can take place through either the photoelastic or the interface deformation mechanisms. The latter has been investigated intensively during the last few years to cool or amplify the mechanical vibrations of a resonator via its coupling to the light. Optomechanical effect at the quantum level may be expected in micro or nanoscale systems hosting both optical and mechanical degrees of freedom. During the last few years, dual phononic–photonic membranes and strip waveguides are proposed to sustain such effects [83, 84]. Finally, more advanced dual phononic–photonic sensors allowing a simultaneous determination of the index of refraction and the acoustic velocity of an embedding liquid can be envisaged [85, 86]. The transmission spectra for each type of waves should display narrow peaks that are sensitive to the corresponding property of the liquid.

Besides the topics related to the existence of absolute band gaps, there is a continuous growing interest on refractive properties of phononic crystals, in particular: negative refraction phenomena and their applications in imaging and sub-wavelength focusing in phononic crystals [87–91], self-collimation and

beam-splitting in relation with the shape of the equifrequency surfaces [92], control of the sound propagation with metamaterials with emphasis on cloaking and hyperlens phenomena.

Thermal transport in nonmetallic nanostructured materials can be strongly affected by the specific phonon dispersion curves as well as by different scattering mechanisms such as phonon–phonon interaction and phonon–boundary scattering which become very important at THz frequencies [93]. The existence of band gaps and flat dispersion curves can reduce the thermal transport and be useful for thermoelectric applications. Different frequency domains of phonons can be involved depending on the temperature and on the wavelength dependent mean free paths. Insights into the latter can be derived from molecular dynamic calculations.

In conclusion, one can expect that the field of phononic crystals will acknowledge a continuous growth in relation with the fundamental understanding of the wave phenomena in these heterogeneous materials and with their numerous expected technological applications. The latter cover a broad range of frequencies from the sonic regime for sound isolation and metamaterial behaviors, to GHz for telecommunications and phonon–photon interaction, and to terahertz for thermal transport phenomena.

References

1. F. Bloch, *Z. Phys.* **52**, 555 (1928)
2. For a review, see E.H. El Boudouti, B. Djafari Rouhani, A. Akjouj, L. Dobrzynski, *Acoustic waves in solids and fluid layered materials. Surf. Sci. Rep.* **64**, 471 (2009)
3. S.M. Rytov, *Sov. Phys. Acoust.* **2**, 6880 (1956)
4. M.M. Sigalas, E.N. Economou, Band structure of elastic waves in two dimensional systems. *Solid State Commun.* **86**, 141 (1993)
5. M.S. Kushwaha, P. Halevi, L. Dobrzynski, B. Djafari-Rouhani, Acoustic band structure of periodic elastic composites. *Phys. Rev. Lett.* **71**, 2022 (1993)
6. M.S. Kushwaha, P. Halevi, L. Dobrzynski, B. Djafari-Rouhani, Theory of acoustic band structure of periodic elastic composites. *Phys. Rev. B* **49**, 2313 (1994)
7. M.M. Sigalas, E.N. Economou, Elastic and acoustic wave band structure. *J. Sound Vib.* **158**, 377 (1992)
8. J.O. Vasseur, B. Djafari-Rouhani, L. Dobrzynski, M.S. Kushwaha, P. Halevi, Complete acoustic band gaps in periodic fibre reinforced composite materials: the carbon/epoxy and some metallic systems. *J. Phys.: Condens. Matter* **7**, 8759–8770 (1994)
9. For a review, see M. Sigalas, M.S. Kushwaha, E.N. Economou, M. Kafesaki, I.E. Psarobas, W. Steurer, Classical vibrational modes in phononic lattices: theory and experiment. *Z. Kristallogr.* **220**, 765–809 (2005)
10. For a recent review, see Y. Pennec, J. Vasseur, B. Djafari Rouhani, L. Dobrzynski, P.A. Deymier, Two-dimensional phononic crystals: examples and applications. *Surf. Sci. Rep.* **65**, 229 (2010)
11. E. Yablonovitch, Inhibited spontaneous emission in solid-state physics and electronics. *Phys. Rev. Lett.* **58**, 2059–2062 (1987)
12. J.D. Joannopoulos, R.D. Meade, J.N. Winn, *Molding the Flow of Light* (Princeton University Press, Princeton, 1995)

13. I.E. Psarobas, A. Modinos, R. Sainidou, N. Stefanou, Acoustic properties of colloidal crystals. *Phys. Rev. B* **65**, 064307 (2002)
14. R. Sainidou, N. Stefanou, A. Modinos, Formation of absolute frequency gaps in three-dimensional solid phononic crystals. *Phys. Rev. B* **66**, 212301 (2002)
15. T. Still, W. Cheng, M. Retsch, R. Sainidou, J. Wang, U. Jonas, N. Stefanou, G. Fytas, Simultaneous occurrence of structure-directed and particle-resonance-induced phononic gaps in colloidal films. *Phys. Rev. Lett.* **100**, 194301 (2008)
16. C. Croëne, E.J.S. Lee, H. Hu, J.H. Page, Band gaps in phononic crystals: generation mechanisms and interaction effects. *AIP Adv.* **1**, 041401 (2011)
17. Z. Liu, X. Zhang, Y. Mao, Y.Y. Zhu, Z. Yang, C.T. Chan, P. Sheng, Locally resonant sonic materials. *Science* **289**, 1734–1736 (2000)
18. M. Torres, F.R. Montero de Espinosa, D. Garcia-Pablos, N. Garcia, Sonic band gaps in finite elastic media: surface states and localization phenomena in linear and point defects. *Phys. Rev. Lett.* **82**, 3054 (1999)
19. M. Kafesaki, M.M. Sigalas, N. Garcia, Frequency modulation in the transmittivity of wave guides in elastic-wave band-gap materials. *Phys. Rev. Lett.* **85**, 4044 (2000)
20. A. Khelif, B. Djafari-Rouhani, J.O. Vasseur, P.A. Deymier, P. Lambin, L. Dobrzynski, Transmittivity through straight and stublike waveguides in a two-dimensional phononic crystal. *Phys. Rev. B* **65**, 174308 (2002)
21. A. Khelif, B. Djafari-Rouhani, J.O. Vasseur, P.A. Deymier, Transmission and dispersion relations of perfect and defect-contained waveguide structures in phononic band gap materials. *Phys. Rev. B* **68**, 024302 (2003)
22. A. Khelif, B. Djafari-Rouhani, V. Laude, M. Solal, Coupling characteristics of localized phonons in photonic crystal fibers. *J. Appl. Phys.* **94**, 7944–7946 (2003)
23. A. Khelif, A. Choujaa, B. Djafari-Rouhani, M. Wilm, S. Ballandras, V. Laude, Trapping and guiding of acoustic waves by defect modes in a full band-gap ultrasonic crystal. *Phys. Rev. B* **68**, 214301 (2003)
24. A. Khelif, A. Choujaa, S. Benchabane, B. Djafari-Rouhani, V. Laude, Guiding and bending of acoustic waves in highly confined phononic crystal waveguides. *Appl. Phys. Lett.* **84**, 4400 (2004)
25. S. Benchabane, A. Khelif, A. Choujaa, B. Djafari-Rouhani, V. Laude, Interaction of waveguide and localized modes in a phononic crystal. *Europhys. Lett.* **71**, 570 (2005)
26. Y. Pennec, B. Djafari Rouhani, J.O. Vasseur, H. Larabi, A. Khelif, A. Choujaa, S. Benchabane, V. Laude, Acoustic channel drop tunneling in a phononic crystal. *Appl. Phys. Lett.* **87**, 261912 (2005)
27. J.O. Vasseur, P.A. Deymier, G. Frantzikonis, G. Hong, B. Djafari Rouhani, L. Dobrzynski, Experimental evidence for the existence of absolute acoustic band gaps in two-dimensional periodic composite media. *J. Phys.: Condens. Matter* **10**, 6051 (1998)
28. J.O. Vasseur, P.A. Deymier, B. Chenni, B. Djafari-Rouhani, L. Dobrzynski, D. Prevost, Experimental and theoretical evidence for the existence of absolute acoustic band gaps in two-dimensional solid phononic crystals. *Phys. Rev. Lett.* **86**, 3012 (2001)
29. F.R. Montero de Espinosa, E. Jimenez, M. Torres, Ultrasonic band gap in a periodic two-dimensional composite. *Phys. Rev. Lett.* **80**, 1208 (1998)
30. H. Larabi, Y. Pennec, B. Djafari-Rouhani, J.O. Vasseur, Multicoaxial cylindrical inclusions in locally resonant phononic crystals. *Phys. Rev. E* **75**, 066601 (2007)
31. E.N. Economou, M.M. Sigalas, Classical wave propagation in periodic structures: cermet versus network topology. *Phys. Rev. B* **48**, 13434 (1993)
32. M.M. Sigalas, E.N. Economou, Attenuation of multiple-scattered sound. *Europhys. Lett.* **36**, 241 (1996)
33. M.S. Kushwaha, Stop-bands for periodic metallic rods: sculptures that can filter the noise. *Appl. Phys. Lett.* **70**, 3218 (1997)
34. P. Lambin, A. Khelif, J.O. Vasseur, L. Dobrzynski, B. Djafari-Rouhani, Stopping of acoustic waves by sonic polymer-fluid composites. *Phys. Rev. E* **63**, 066605 (2001)

35. J.O. Vasseur, P.A. Deymier, A. Khelif, P. Lambin, B. Djafari-Rouhani, A. Akjouj, L. Dobrzynski, N. Fettouhi, J. Zemmouri, Phononic crystal with low filling fraction and absolute acoustic band gap in the audible frequency range: a theoretical and experimental study. *Phys. Rev. E* **65**, 056608 (2002)
36. Z. Liu, C.T. Chan, P. Sheng, A.L. Goertzen, J.H. Page, Elastic wave scattering by periodic structures of spherical objects: theory and experiment. *Phys. Rev. B* **62**, 2446 (2000)
37. J.H. Page, A.L. Goertzen, S. Yang, Z. Liu, C.T. Chan, P. Sheng, in *Photonic Crystals and Light Localization in the 21st Century*, ed. by C.M. Soukoulis (Kluwer, Dordrecht, 2001), p. 59
38. M.S. Kushwaha, B. Djafari-Rouhani, Complete acoustic stop bands for cubic arrays of spherical liquid balloons. *J. Appl. Phys.* **80**, 3191 (1996)
39. R. Martinez-Sala, J. Sancho, J.V. Sanchez, V. Gomez, J. Llinares, F. Meseguer, Sound attenuation by sculpture. *Nature* **378**, 241 (1995)
40. D. Caballero, J. Sanchez-Dehesa, C. Rubio, R. Martinez-Sala, J.V. Sanchez-Perez, F. Meseguer, J. Llinares, Large two-dimensional sonic band gaps. *Phys. Rev. E* **60**, 6316 (1999)
41. Y. Pennec, B. Djafari-Rouhani, J. Vasseur, P.A. Deymier, A. Khelif, Tunable filtering and demultiplexing in phononic crystals with hollow cylinders. *Phys. Rev. E* **69**, 046608 (2004)
42. J.V. Sanchez-Pérez, D. Caballero, R. Martínez-Sala, C. Rubio, J. Sánchez-Dehesa, F. Meseguer, J. Llinares, F. Gálvez, Sound attenuation by a two-dimensional array of rigid cylinders. *Phys. Rev. Lett.* **80**, 5325 (1998)
43. Y. Pennec, B. Djafari-Rouhani, J.O. Vasseur, P.A. Deymier, A. Khelif, Transmission and dispersion modes in phononic crystals with hollow cylinders: application to waveguide structure. *Phys. Stat. Sol. (c)* **1**(11), 2711–2715 (2004)
44. A. Sato, W. Knoll, Y. Pennec, B. Djafari-Rouhani, G. Fytas, M. Steinhart, Anisotropic propagation and confinement of high frequency phonons in nanocomposites. *J. Chem. Phys.* **130**, 111102 (2009)
45. R. Lucklum, J. Li, Phononic crystals for liquid sensor applications. *Meas. Sci. Technol.* **20**, 124014 (2009)
46. M. Ke, M. Zubtsov, R. Lucklum, Sub-wavelength phononic crystal liquid sensor. *J. Appl. Phys.* **110**, 026101 (2011)
47. M.S. Kushwaha, B. Djafari-Rouhani, Giant sonic stop bands in two-dimensional periodic system of fluids. *J. Appl. Phys.* **84**, 4677 (1998)
48. M.S. Kushwaha, B. Djafari Rouhani, L. Dobrzynski, Sound isolation from cubic arrays of air bubbles in water. *Phys. Lett. A* **248**, 252–256 (1998)
49. V. Leroy, A. Bretagne, M. Fink, H. Willaime, P. Tabeling, A. Tourin, Design and characterization of bubble phononic crystals. *Appl. Phys. Lett.* **95**, 171904 (2009)
50. T. Still, M. Oudich, G.K. Auernhammer, D. Vlassopoulos, B. Djafari-Rhouani, G. Fytas, P. Sheng, Soft silicone rubber in phononic structures: correct elastic moduli. *Phys. Rev. B* **88**, 094102 (2013)
51. C. Goffaux, J.P. Vigeron, Theoretical study of a tunable phononic band gap system. *Phys. Rev. B* **64**, 075118 (2001)
52. M. Torres, F.R. Montero de Espinosa, J.L. Aragon, Ultrasonic wedges for elastic wave bending and splitting without requiring a full band gap. *Phys. Rev. Lett.* **86**, 4282 (2001)
53. J.O. Vasseur, P.A. Deymier, M. Beaugeois, Y. Pennec, B. Djafari-Rouhani, D. Prevost, Experimental observation of resonant filtering in a two-dimensional phononic crystal waveguide. *Z. Kristallogr.* **220**, 824 (2005)
54. B. Djafari Rouhani, L. Dobrzynski, O. Hardouin Duparc, R.E. Camley, A.A. Maradudin, Sagittal elastic waves in infinite and semi-infinite superlattices. *Phys. Rev. B* **28**, 1711 (1983)
55. B. Djafari Rouhani, A.A. Maradudin, R.F. Wallis, Rayleigh waves on a superlattice stratified normal to the surface. *Phys. Rev. B* **29**, 6454 (1984)
56. Y. Tanaka, S. Tamura, Surface acoustic waves in two-dimensional periodic elastic structures. *Phys. Rev. B* **58**, 7958 (1998) and Acoustic stop bands of surface and bulk modes in two-dimensional phononic lattices consisting of aluminum and a polymer. *Phys. Rev. B* **60**, 13294 (1999)

57. T.-T. Wu, Z.-G. Huang, S. Lin, Surface and bulk acoustic waves in two-dimensional phononic crystals consisting of materials with general anisotropy. *Phys. Rev. B* **69**, 094301 (2004)
58. T.-T. Wu, L.-C. Wu, Z.-G. Huang, Frequency band-gap measurement of two-dimensional air/silicon phononic crystals using layered slanted finger interdigital transducers. *J. Appl. Phys.* **97**(094916) (2005)
59. S. Benchabane, A. Khelif, J.-Y. Rauch, L. Robert, V. Laude, Evidence for complete surface wave band gap in a piezoelectric phononic crystal. *Phys. Rev. E* **73**, 065601 (2006)
60. B. Bonello, C. Charles, F. Ganot, Velocity of a SAW propagating in a 2D phononic crystal. *Ultrasonics* **44**, 1259–1263 (2006)
61. S. Benchabane, O. Gaiffe, R. Salut, G. Ulliac, Y. Achaoui, V. Laude, Observation of surface-guided waves in holey hypersonic phononic crystal. *Appl. Phys. Lett.* **98**, 171908 (2011)
62. V. Laude, M. Wilm, S. Benchabane, A. Khelif, Full band gap for surface acoustic waves in a piezoelectric phononic crystal. *Phys. Rev. E* **71**, 036607 (2005)
63. B. Manzanera-Martinez, F. Ramos-Mendieta, Surface elastic waves in solid composites of two-dimensional periodicity. *Phys. Rev. B* **68**, 134303 (2003)
64. R. Sainidou, B. Djafari Rouhani, J.O. Vasseur, Surface acoustic waves in finite slabs of three-dimensional phononic crystals. *Phys. Rev. B* **77**, 094304 (2007)
65. A. Khelif, B. Aoubiza, S. Mohammadi, A. Adibi, V. Laude, Complete band gaps in two-dimensional phononic crystal slabs. *Phys. Rev. E* **74**, 046610 (2006)
66. J.O. Vasseur, P. Deymier, B. Djafari Rouhani, Y. Pennec, A.C. Hladky-Hennion, Absolute forbidden bands and waveguiding in two-dimensional phononic crystal plates. *Phys. Rev. B* **77**, 085415 (2008)
67. Y. Pennec, B. Djafari Rouhani, H. Larabi, J. Vasseur, A.C. Hladky-Hennion, Low frequency gaps in a phononic crystal constituted of cylindrical dots deposited on a thin homogeneous plate. *Phys. Rev. B* **78**, 104105 (2008)
68. T.T. Wu, Z.G. Huang, T.-C. Tsai, T.C. Wu, Evidence of complete band gap and resonances in a plate with periodic stubbed surface. *Appl. Phys. Lett.* **93**, 111902 (2008)
69. T.C. Wu, T.T. Wu, J.C. Hsu, Waveguiding and frequency selection of Lamb waves in a plate with a periodic stubbed surface. *Phys. Rev. B* **79**, 104306 (2009)
70. Y. Pennec, B. Djafari Rouhani, H. Larabi, A. Akjouj, J.N. Gillet, J.O. Vasseur, G. Thabet, Phonon transport and waveguiding in a phononic crystal made up of cylindrical dots on a thin homogeneous plate. *Phys. Rev. B* **80**, 144302 (2009)
71. S. Mohammadi, A.A. Eftekhari, W.D. Hunt, A. Adibi, High-Q micromechanical resonators in a two-dimensional phononic crystal slab. *Appl. Phys. Lett.* **94**, 051906 (2009)
72. C.M. Reinke, M.F. Su, R.H. Olsson, I. El-Kady, Realization of optimal bandgaps in solid–solid, solid–air, and hybrid solid–air–solid phononic crystal slabs. *Appl. Phys. Lett.* **98**, 061912 (2011)
73. Z. Hou, F. Wu, Y. Liu, Phononic crystals containing piezoelectric material. *Solid State Commun.* **130**(11), 745–749 (2004)
74. X.-Y. Zou, Q. Chen, B. Liang, J.-C. Cheng, Control of the elastic wave bandgaps in two-dimensional piezoelectric periodic structures. *Smart Mater. Struct.* **17**, 015008 (2008)
75. Y.-Z. Wang, F.-M. Li, K. Kishimoto, Y.-S. Wang, W.-H. Huang, Elastic wave band gaps in magneto-electrostatic phononic crystals. *Wave Motion* **46**(47) (2009)
76. J.-F. Robillard, O. Bou Matar, J.O. Vasseur, P.A. Deymier, M. Stippinger, A.C. Hladky-Hennion, Y. Pennec, B. Djafari-Rouhani, Tunable magnetoelastic phononic crystals. *Appl. Phys. Lett.* **95**, 124104 (2009)
77. K. Bertoldi, M.C. Boyce, Mechanically triggered transformations of phononic band gaps in periodic elastomeric structures. *Phys. Rev. B* **77**, 052105 (2008)
78. Z.-G. Huang, T.-T. Wu, Temperature effect on the bandgaps of surface and bulk acoustic waves in two-dimensional phononic crystals. *IEEE Trans. Ultrason. Ferroelectr. Freq. Contr.* **52**, 365 (2005)
79. A. Sato, Y. Pennec, N. Shingne, T. Thurn-Albrecht, W. Knoll, M. Steinhart, B. Djafari-Rouhani, G. Fytas, Tuning and switching the hypersonic phononic properties of elastic impedance contrast nanocomposites. *ACS Nano* **4**, 3471 (2010)

80. M. Maldovan, E.L. Thomas, Simultaneous localization of photons and phonons in two-dimensional periodic structures. *Appl. Phys. Lett.* **88**, 251907 (2006)
81. S. Mohammadi, A.A. Eftekhari, A. Khelif, A. Adibi, Simultaneous two-dimensional phononic and photonic band gaps in opto-mechanical crystal slabs. *Opt. Express* **18**, 9164 (2010)
82. Y. Pennec, B. Djafari-Rouhani, E.H. El Boudouti, C. Li, Y. El Hassouani, J.O. Vasseur, N. Papanikolaou, S. Benchabane, V. Laude, A. Martinez, Simultaneous existence of phononic and photonic band gaps in periodic crystal slabs. *Opt. Express* **18**, 14301 (2010)
83. M. Eichenfield, J. Chan, R.M. Camacho, K.J. Vahala, O. Painter, Optomechanical crystals. *Nature* **462**, 78 (2009)
84. Y. Pennec, B. Djafari-Rouhani, C. Li, J.M. Escalante, A. Martinez, S. Benchabane, V. Laude, N. Papanikolaou, Band gaps and cavity modes in dual phononic and photonic strip waveguides. *AIP Adv.* **1**, 041901 (2011)
85. S. Amoudache, Y. Pennec, B. Djafari Rouhani, A. Khater, R. Lucklum and R. Tigrine, Simultaneous sensing of light and sound velocities of fluids in a two-dimensional phoXonic crystal with defects, *J. Appl. Phys.* **115**, 134503 (2014)
86. R. Lucklum, Y. Pennec, A. Kraych, M. Zubstov, B. Djafari Rouhani, in *Phoxonic Crystal Sensor*, SPIE Photonics Europe, Photonic Crystal Materials and Devices X, Brussels, Belgium, April 16–19, 2012, *Proc. SPIE-Int. Soc. Opt. Eng.*, 8425 (2012) 84250N-1-8, ISBN 978-0-8194-9117-6. doi:[10.1117/12.922553](https://doi.org/10.1117/12.922553)
87. S. Yang, J.H. Page, Z. Liu, M.L. Cowan, C.T. Chan, P. Sheng, Focusing of sound in a 3D phononic crystal. *Phys. Rev. Lett.* **93**, 024301 (2004)
88. K. Imamura, S. Tamura, Negative refraction of phonons and acoustic lensing effect of a crystalline slab. *Phys. Rev. B* **70**, 174308 (2004)
89. X. Zhang, Z. Liu, Negative refraction of acoustic waves in two-dimensional phononic crystals. *Appl. Phys. Lett.* **85**, 341 (2004)
90. A. Sukhovich, L. Jing, J.H. Page, Negative refraction and focusing of ultrasound in two-dimensional phononic crystals. *Phys. Rev. B* **77**, 014301 (2008)
91. A. Sukhovich, B. Merheb, K. Muralidharan, J.O. Vasseur, Y. Pennec, P.A. Deymier, J.H. Page, Experimental and theoretical evidence for subwavelength imaging in phononic crystals. *Phys. Rev. Lett.* **102**, 154301 (2009)
92. J. Bucay, E. Roussel, J.O. Vasseur, P.A. Deymier, A.-C. Hladky-Hennion, Y. Pennec, K. Muralidharan, B. Djafari-Rouhani, B. Dubus, Positive, negative, zero refraction, and beam splitting in a solid/air phononic crystal: theoretical and experimental study. *Phys. Rev. B* **79**(214305) (2009)
93. P.E. Hopkins, C.M. Reinke, M.F. Su, R.H. Olsson III, E.A. Shaner, Z.C. Leseman, J.R. Serrano, L.M. Phinney, I. El-Kady, Reduction in the thermal conductivity of single crystalline silicon by phononic crystal patterning. *Nano Lett.* **11**, 107 (2011)

Phononic Crystals

Fundamentals and Applications

Khelif, A.; Adibi, A. (Eds.)

2016, VII, 245 p. 129 illus., 88 illus. in color., Hardcover

ISBN: 978-1-4614-9392-1